A model for measurement of the states in a coupled-dot qubit

H B Sun and H M Wiseman

Centre for Quantum Computer Technology, Centre for Quantum Dynamics, Griffith University, Brisbane 4111 QLD Australia

E-mail: h.sun@griffith.edu.au

Abstract. We propose a quantum trajectory analysis of a scheme to measure the states of a coupled dot device (qubit) where there is a fluctuating energy gap Δ between the two states. The system consists of the qubit and a readout dot coupled to source and drain leads. The tunnel rate through the detector is conditioned by the occupation number of the nearer quantum dot (target) of the qubit and therefore probes the states of the qubit. We derive a Lindblad-form master equation to calculate the unconditional evolution of the qubit and a conditional stochastic master equation calculating the conditional evolution for different tunneling rates. The results show the effects of various device parameters and provide the optimum selection and combination of the system structure.

1. Introduction

There have been wide interests and numerous proposals in the area of quantum transport and measurement in mesoscopic electronic system [1-11]. Coupled quantum dots have been suggested as qubits: the basic element of a quantum computer. In addition to manipulations of quantum states, a readout device is required to perform quantum measurements of the resulting state of the qubit. The accurate readout of data encoded in the qubit states is an important part of the performance of a quantum computer. In this paper, we analyse a method to measure the states of a coupled dot qubit based on the theory of open quantum system [12]. The measurement postulate of quantum mechanics states requires that the unitary quantum evolution to be applied to the total system, which includes the measurement apparatus and the measured system. However the measurement process automatically introduces a statistical description of the system dynamics. A density matrix describing a pure state has the property: $\rho^2 = \rho$, which is not the case for a density matrix describing a statistical ensemble. The Lindblad equation [13] is the quantum master equation of the reduced dynamics that still preserve the three basic properties of the density matrix: positivity, Hermitivity and the norm required to describe a pure state, as well as markoviaity describing a subsystem that undergoes an irreversible dynamics to equilibrium. The whole system in this study includes a measurement device of a quantum tunneling readout-detector (RD) such as the quantum contact point, single electron transistor, or quantum dot coupled to source and drain leads, and a coupled-quantum dot of the charge qubit as the system being measured. We derive a conditional stochastic master equation to describe the conditioned evolution of the qubit. The ensemble-averaged evolution of the qubit state is calculated for various parameter combinations to estimate the optimum selection.

In section 2 we introduce the system and modeling followed by section 3 calculating trajectories in the cases of without and with variable energy gap between two dot states. We discuss the results in section 4 and summarize in section 5.

2. The System and modeling

The system studied is depicted schematically in figure 1. There is a single electronic bound state that can be occupied in each dot of the qubit. The energy difference between these two bound states is Δ and the electron can tunnel between two dots at rate t. In the RD, the electron-tunneling rate is conditioned on the occupation of the nearer dot (target) at D_{θ} and $D_{\theta}+D_{I}$ for non-occupied and occupied cases respectively.

Figure 1 Illustration of the system

The total Hamiltonian of the qubit system for coherent coupling case ($\Delta = 0$) is

$$H = \hbar \sum_{i=1}^{2} \omega_{i} c_{i}^{\dagger} c_{i} + i\hbar \frac{t}{2} (c_{1}^{\dagger} c_{2} - c_{2}^{\dagger} c_{1})$$
 (1)

where c_i^{\dagger}, c_i represent the Fermi annihilation and creation operators for the single electron state of the *ith* dot and *t* is the tunneling rate between two dot states. For the readout dot, the background tunnelling current, when the target is not occupied, is D_0 , and the rate of the detected signal of the occupation of the target is $D_0 + D_I$ with $D_I > 0$. We assume that the tunneling through the RD is one way only (\downarrow direction as shown in figure 1) and the escaping tunneling rate is large compared to other rates and based on these we can derive a Lindblad-form master equation [4]:

$$\frac{d\rho}{dt} = -i\left[H,\rho\right] + \gamma_{dec}\left\{c_1^{\dagger}c_1\rho c_1^{\dagger}c_1 - \frac{1}{2}\left[c_1^{\dagger}c_1c_1^{\dagger}c_1\rho + \rho c_1^{\dagger}c_1c_1^{\dagger}c_1\right]\right\}$$

where $\gamma_{dec} = 2D_0 + D_1$ is the decoherence rate. The stochastic record of measurement comprises a sequence of times at which electrons tunnel through the RD. In the zero response-time limit, the current consists of a

sequence of δ function spikes: i(t) = edN/dt where dN(t) is a classical point process defined by the following conditions

$$\left[dN(t) \right]^2 = dN(t)$$

$$E \left[dN(t) \right] / dt = D_0 + D_1 Tr \left[c_1^{\dagger} c_1 \rho_c(t) c_1^{\dagger} c_1 \right]$$
(2)

where E[x] indicates a classical average of a classical stochastic process x. The first condition states that dN(t) equals zero or one. The second means that the rate of events is equal to the quiescent rate D_0 plus an additional rate D_I if and only if the electron is in the target dot. Applying the theory of open quantum systems [12], we obtain the stochastic master equation conditioned on the observed event in time dt as [4]

$$d\rho_{c} = dN \left[\frac{D_{0} + D_{1}7[c_{1}^{\dagger}c_{1}] + 2D_{0}\mathcal{D}[c_{1}^{\dagger}c_{1}]}{D_{0} + D_{1}Tr[\rho_{c}c_{1}^{\dagger}c_{1}]} - 1 \right] \rho_{c} + dt \left[\frac{-D_{1}}{2} \left\{ c_{1}^{\dagger}c_{1}, \rho_{c} \right\} + D_{1}Tr[\rho_{c}c_{1}^{\dagger}c_{1}] \rho_{c} - i[H, \rho_{c}] \right]$$
(3)

 $7[A]B = ABA^{\dagger}, \{A,B\} = AB + BA$ where and

 $\mathcal{D}[A]B = \mathcal{T}[A]B - (A^{\dagger}AB + BA^{\dagger}A) / 2.$

3. Calculations

3.1 Coherent tunneling case

To simplify the calculations we introduce the Bloch representation of the state matrix:

$$\rho = \frac{1}{2} \left(I + x \sigma_x + y \sigma_y + z \sigma_z \right) \tag{4}$$

The Pauli matrices are defined as

$$\sigma_x = c_1^{\dagger} c_2 + c_2^{\dagger} c_1, \quad \sigma_y = i \left(c_2^{\dagger} c_1 - c_1^{\dagger} c_2 \right), \quad \sigma_z = c_2^{\dagger} c_2 - c_1^{\dagger} c_1$$
 (5)

The moments of the Pauli matrices are given by $\langle \sigma_{\alpha} \rangle = \alpha$ ($\alpha = x, y, z$), which provide physical meanings. For example, when the system is in a definite state (dot 1 or dot 2), the average population difference z is equal to ±1. The set of coupled stochastic differential equations for the Bloch sphere variables can be expressed as:

$$\begin{cases} dx_{c} = \left(-tZ_{c} - \frac{D_{1}}{2}z_{c}x_{c}\right)dt - x_{c}dN(t), \\ dy_{c} = -\frac{D_{1}}{2}z_{c}y_{c}dt - y_{c}dN(t), \\ dz_{c} = \left[tx_{c} + \frac{D_{1}}{2}(1 - z_{c}^{2})\right]dt - \left[\frac{D_{1}(1 - z_{c}^{2})/2}{D_{0} + D_{1}(1 - z_{c}^{2})/2}\right] \end{cases}$$
(6)

Detailed derivation and approximation are referred in ref. [4]. The subscript c indicates that these variables refer to the conditional state. Calculated the trajectories at various coupling rates when $D_0=0$ are plotted in figure 2. When the coupling between the dots is small ($t < \gamma_{\rm dec}/2$) the electron is located in a fixed dot (z=-1 at dot 2 and z=+1 at dot 1) for a long time till a sudden transition as shown in figure 2(a). For strong coupling case, as shown in figure 2(c) when $t > \gamma_{\rm dec}/2$, the trajectory shows nearly sinusoidal oscillations with jumps occurring at an average rate of $\gamma_{\rm dec}/2$, this means that the electron is not localized but shared by two dots through the strong tunnelling. In figure 2 (b), with the moderate coupling strength, the trajectory shows that the electron is neither well localized nor regular harmonically oscillating between two dots.

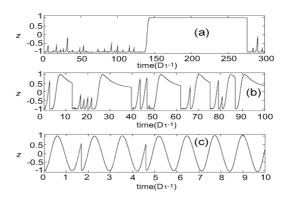


Figure 2 Trajectories for various coupling rates: $t = (a) \ 0.1$; (b) 0.5; and (c) 5 D_L .

3.1 Energy gap $\Delta \neq 0$ case

We extend the application to the case that there is an energy difference of $\Delta \neq 0$ between two dot states, which is a model of, for example, the qubit system proposed by Kane [14]. The relevant Hamiltonian can be written as $H = \begin{pmatrix} \Delta & t \\ t & 0 \end{pmatrix}$, where t is the tunnelling between two states. The stochastic

differential equations for the Bloch sphere variables describing conditional dynamics now become:

$$\begin{cases} dx_{c} = \left(-tz_{c} - y_{c}\Delta - \frac{D_{1}}{2}x_{c}z_{c}\right)dt - x_{c}dN(t) \\ dy_{c} = \left(x_{c}\Delta - \frac{D_{1}}{2}y_{c}z_{c}\right)dt - y_{c}dN(t) \\ dz_{c} = \left(tx_{c} + \frac{D_{1}}{2}\left(1 - z_{c}^{2}\right)\right)dt - \frac{D_{1}\left(1 - z_{c}^{2}\right)/2}{D_{0} + D_{1}\left(1 - z_{c}^{2}\right)/2}dN(t) \end{cases}$$

$$(7)$$

The numerical calculation results are presented in figure 3. By comparison with figure 2 one can see the effect of the energy gap. It takes much longer time to tunnel through the gap from one dot to the other for the low tunneling rate case (note: the time scales on the horizontal axes are

different in these two figures) while quasi-harmonic oscillation features are kept in high tunneling rate region (tunneling rate >> gap Δ). For the moderate coupling rate the plot shows none-localization and non-sinusoidal oscillations between two dots with lower frequency compared to those in figure 2.

In order to investigate the influences of various parameters of devices on the system dynamics (performance) we investigate the unconditional ensemble average properties of the system in detail.

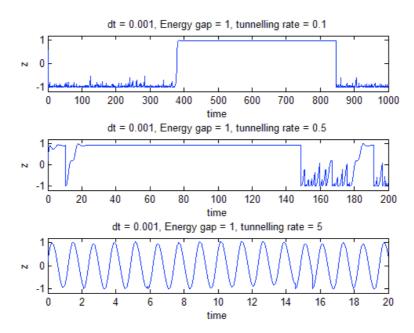


Figure 3 Trajectories for various t with $\Delta = 1$, the parameters are shown on top of each plot and the rates are all normalized by D_1 .

3.3 Ensemble average properties

The relevant Hamiltonian can be diagonalized by rotating an angle of $\theta = \frac{1}{2} t g^{-1} \left(\frac{2t}{\Delta} \right)$ to $\tilde{H} = \begin{pmatrix} \alpha & 0 \\ 0 & \beta \end{pmatrix}$

with
$$\alpha = \frac{1}{2} \left(\Delta + \sqrt{\Delta^2 + 4t^2} \right); \quad \beta = \frac{1}{2} \left(\Delta - \sqrt{\Delta^2 + 4t^2} \right)$$
 (8)

the transformation from the original representation to the new representation is given by:

$$\begin{pmatrix} \tilde{x} \\ \tilde{y} \\ \tilde{z} \end{pmatrix} = \begin{pmatrix} \cos(2\theta) & 0 & \sin(2\theta) \\ 0 & 1 & 0 \\ -\sin(2\theta) & 0 & \cos(2\theta) \end{pmatrix} \begin{pmatrix} x \\ y \\ z \end{pmatrix}$$

In the new representation, the evolution of the ensemble-averaged Bloch sphere variables is described by

$$\begin{pmatrix} \ddot{x} \\ \dot{\ddot{y}} \\ \dot{\ddot{z}} \end{pmatrix} = \begin{pmatrix} \frac{-\gamma_{dec}}{2} \cos^2(2\theta) & \sqrt{\Delta^2 + 4t^2} & \frac{-\gamma_{dec}}{4} \sin(4\theta) \\ -\sqrt{\Delta^2 + 4t^2} & \frac{-\gamma_{dec}}{2} & 0 \\ \frac{-\gamma_{dec}}{4} \sin(4\theta) & 0 & \frac{-\gamma_{dec}}{2} \sin^2(4\theta) \end{pmatrix} \begin{pmatrix} \tilde{x} \\ \tilde{y} \\ \tilde{z} \end{pmatrix}$$
 (9)

We can monitor the state of the qubit from the evolution of the moment z(t). The calculated results of ensemble-averaged evolution of the system state are plotted in figures 4 - 8 illustrating the influence of various parameters. When a particular parameter is chosen to vary in a plot, all other parameters in the figure are fixed.

4. Results and discussion

For the ensemble evaluation of the qubit state we use the approximate values of real Δ and t given by Kane [14], ie. $\Delta/h = 110$ GHz and 2t/h = 1GHz. The values of the ratio of t/Δ in all plots are therefore chosen as 5×10^{-3} .

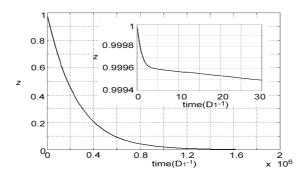


Figure 4 Locality of the electron at $D_0 = 0.5$, $\Delta = 0.1$ and $t = 10^{-4} D_1$.

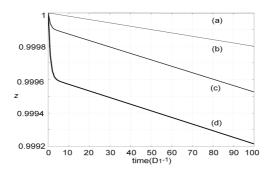


Figure 5 Influence of Δ : from top $\Delta = 10, 5, 0.2, 0.1 D_1$.

Figure 4 shows a typical evolution of the locality of the state. It is obvious that the system is not oscillating but deviates from the initial state to a mixed state as time approaches "infinity", which is different from the coherent tunneling case. The insert is enlarged details of the early stage, which shows a sharp deviation followed a flatter slope. Figures 5-7 show

the effects of the energy gap Δ , the coupling rate between the two dotes t and the quiescent rate of current tunneling through the RD D_{θ} respectively.

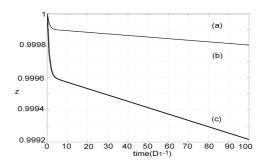


Figure 6 Influence of *t*, from top: $t = 10^{-4}$, $5 \times 10^{-4} D_1$

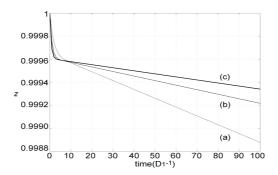


Figure 7 Influence of D_0 : from top $D_0 = 0$, 0.5, 1 D_1 .

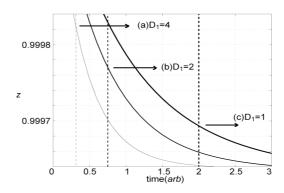


Figure 8 Comparison of measurement quality for various D_I . The dashed lines are corresponding characteristic times.

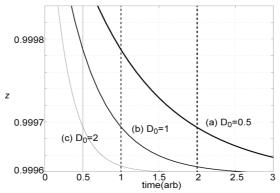


Figure 9 Comparison of measurement quality for different values of D_0 at a fixed ratio of $D_0/D_1 = 0.5$.

In the plots all parameters are normalized by the rate D_I . Both top lines (a) in figure 6 and figure 8 are very close to the top frame edge. As expected, we see that the larger Δ (figure 5 (a)) and the smaller t (figure 6 (a)), the slower deviation and the smaller background rate of the detector D_{θ} ((c) in figure 7), the better measurement quality. The interesting feature in figure 7 is that with a small D_0 , z(t) shows a sharp first slope followed a flatter second slope, which is most desirable condition, as it may be interpreted as that the state is distinguished quickly with less deviation from the initial state. Now we reach a question naturally: how would one judge the quality of a measurement? One parameter determining the quality of a measurement is the localisation rate, which is related to the signal-to-noise ratio. The characteristic time is defined as the minimum time when the two possibilities of the electron locality are distinguishable. In our system it is given by $T = (2D_0 + D_1)/D_1^2$, which is twice inverse of the localisation rate [4]. Within the characteristic time the closer to the initial state, the better measurement. Figures 8 and 9 illustrate the comparisons of the measurement qualities with various parameter combinations. Figure 8 shows that the larger D_1 (strong coupling between the qubit and the detector), the more sensitive detection, the RD reads out the state of the qubit in a shorter time with less disturbance. In figure 9, D_0 and D_1 vary in their absolute values at the fixed ratio of $D_0/D_1 = 0.5$. It is clear from the graph that the larger rates of RD (curve c) make better measurement and strong coupling is therefore preferred. The above outcomes may provide reference for the device designers when they tackle optimum selection of the parameters. For example if the technology limits the reduction of quiescent current of a non-ideal detector one could increase the measurement tunneling rate D_1 by device designing or bias setting in experiments to compensate and achieve better measurement quality.

5. Summary

It has been suggested to use mesoscopic electronic systems such as coupled quantum dots, superconducting junctions and single spin-polarised electrons as qubits. We model the quantum measurement of states of such systems using the theory of open quantum system. The requirements to perform quantum calculations and a quantum measurement (readout) appear to contradict each other. During the manipulations the dephasing should be minimised, while a quantum

measurement should dephase the state of the qubit as far as possible. We propose a measurement scheme to study the dynamics of the system. To guarantee the calculated evolution representing the state of a real physical system we derive the Lindblad-form master equation. We calculate the conditional evolution of the states and the ensemble-averaged evolution of the states of the coupled quantum dots as the qubit. The results show the effects of various device parameters on the quality of the measurements. These may contribute to the device parameter selection and experimental designing of the readout processes of a solid-state quantum computer for the better performance.

References

- [1] Gurvitz S A 1997 Phys. Rev. B 56, 15215
- [2] Shninman A and Schhon G 1998 Phys. Rev. B 57 15400 (1998)
- [3] Sun H B and Milburn G J 1999 Phys. Rev. B 59, 10748
- [4] Wiseman H M et al 2001 Phys. Rev. B 63 235398
- [5] Korotkov A N 2001 Phys. Rev. B 63 85312
- [6] Gurvitz et al 2003 Phys. Rev. Lett, 91 66801
- [7] Jordan A N and Buttiker M 2005 Phys. Rev. Lett. 95 220401
- [8] Oxtoby N P et al 2006 Phs. Rev. B 74 045328
- [9] Luo J Y at al 2007 Phys. Rev. B 76 085325
- [10] Kieblich G et al Phys. Rev. Lett 2007 99 206602
- [11] Dong B et al 2008 Phys. Rev. B 77, 085309
- [12] Carmichael H, "An Open Systems Approach to Quantum Optics" (Springer Verlag, Berlin, 1993); Wiseman H M and Milburn G J 1993 Phys. Rev. A 47 1652 (appendix)
- [13] Lindblad G Commun. Math. Phys. 48, 119, 1976)
- [14] Kane B E et al 2000 Phys. Rev. B 61, 2961